# Development of an Unsteady Conjugate Heat Transfer Solver for Rotating Detonation Engines

Yuechen Hou, John Z. Ma, Zhaohua Sheng, Jianping Wang*
Center for Combustion and Propulsion, CAPT&SKLTCS, Department of Mechanics and Aerospace Engineering, College of Engineering, Peking University,
Beijing 100871, China

## 1 Introduction

Rotating detonation engines (RDEs) have been at the forefront of detonation engine research owing to its lower entropy generation and potential increase in propulsion performance over traditional engines utilizing deflagration. However, the thermal environment of rotating detonation chamber (RDC) may be more complex and harsh than the traditional engines as well as pulse detonation engine, due to the high temperature up to 3000K of the gas product behind detonation and high-frequency operation. Besides the potentially higher surface temperature and bulk heat flux which are challenging for the combustor cooling strategies design, the unsteady heat transfer associated with high-frequency propagation of detonations can also impose negative effect on the survivability of wall materials and coatings. As a result, the run time of most laboratory RDE are typically restricted in seconds.

Therefore, the unsteady heat transfer in RDC must be quantified before the future practical application. Yet little work has been published on measurement or simulation of transient heat load of rotating detonation chamber wall. The pioneering experimental work of Bykovskii et al. [1] reported that the bulk heat transfer to the RDC walls is greatest at the axial height of detonation waves. Theuerkauf et al. [2] measured high-frequency surface heat flux of RDE using thin resistance temperature detectors, and then compared with simulated heat flux of RDE in a 2D reactive Euler model [3]. With regard to the numerical work, Roy et al. [4] modeled the combustion and wall heating processes separately, utilizing the temperature data from 3D simulation of RDE as the boundary condition for inner chamber wall surface, in order to avoid expensive computational effort. However, the thermal effect from solid wall to fluid cannot be neglected, which can be proved by the impact of isothermal boundary conditions on RDE simulation. Cocks et al. [5] applied an isothermal wall boundary of 800K to represent the wall temperature of a water cooled RDC. They found that the near-wall deflagration burning is suppressed compared with the adiabatic boundary situation, and the shape of detonation front is significantly alterd, which was also observed as so-called boundary oblique detonation (BOD) by Wang et al. [6] in 2D simulation of RDE. Wu et al. [7] applied isothermal wall boundary to consider the heat loss on the wall, and found that the detonation velocity decreased compared with the adiabatic case.

In order to fully couple the fluid-solid heat transfer process in RDE, conjugate heat transfer (CHT) models, i.e., heat conduction in solid region needs to be considered along with heat convection in adjacent fluid region, has to be established. Similar work of Olcucuoglu et al. [8] has proved the

Correspondence to: wangjp@pku.edu.cn 

effectiveness of this method on quatifying the heat load of detonation engines. In this work, a new solver called multiRegionBYRFoam is developed based on our in-house solver BYRFoam to calculate the CHT problem between the RDC flow field and chamber wall, with the aim of studying the unsteady thermal environment in RDE, evaluating the wall surface temperature and wall heat flux, as well as understanding the thermal effects of chamber wall on detonation propagation and engine performance.

## 2 Methodology

### A. Governing Equations

To begin with, the three-dimensional compressible Navier-Stokes equations solving for detonation in fluid region is given below. It should be stated that the turbulence model is not adopted in this preliminary study, with the consideration that the current turbulent theory for detonation is still limited and may cause inaccurate results. The turbulence models will be tested in our future work, after inspecting the results of laminar heat transfer simulation and compared with experimental data.

$$\frac{\partial \rho}{\partial t} + \nabla \cdot [\rho \vec{U}] = 0, \tag{1}$$

$$\frac{\partial (\rho \vec{U})}{\partial t} + \nabla \cdot \left[\vec{U}\left(\rho \vec{U}\right)\right] + \nabla p + \nabla \cdot \sigma = 0, \tag{2}$$

$$\frac{\partial \rho Y_i}{\partial t} + \nabla \cdot [\rho \vec{U} Y_i] = \dot{\omega}_i, \tag{3}$$

$$\frac{\partial (\rho e_s)}{\partial t} + \nabla \cdot \left[\vec{U}(\rho e_s)\right] + \nabla \cdot [\vec{U} p] + \nabla \cdot (\sigma \cdot \vec{U}) + \nabla \cdot j = \dot{\omega}, \tag{4}$$

where $Y_i$ and $\dot{\omega}_i$ represent the mass fraction and reaction rate of the $i$th species, respectively. The viscous stress tensor $\sigma$ in Eq. (2), the specific total sensible energy $e_s$, the diffusive flux of heat $j$, and the heat release rate $\dot{\omega}$ due to chemical reactions in Eq. (4) are given by

$$\sigma = -\mu\left[\nabla \vec{U} + (\nabla \vec{U})^T - 2/3(\nabla \cdot \vec{U})I\right], \tag{5}$$

$$e_s = e + \left|\vec{U}\right|^2/2 - \sum_{i=1}^{N} Y_i \Delta h_{f,i}^o, \tag{6}$$

$$j = -\alpha_{eff} \nabla e, \tag{7}$$

$$\dot{\omega} \equiv -\sum_{i=1}^{N} \dot{\omega}_i \Delta h_{f,i}^o, \tag{8}$$

where $\mu$ is the dynamic viscosity, $e$ represents the specific internal energy, and $\Delta h_{f,i}^o$ represents the mass-based enthalpy of formation of the $i$th species. The effective thermal diffusivity of the fluid, $\alpha_{eff}$, is the sum of laminar and turbulent thermal diffusivities, and equals to laminar thermal diffusivity in laminar situation. Throughout the solid domain, only the heat conduction laplacian equation will be solved, which can be expressed as follows with the radiative heat transfer neglected.

$$\frac{\partial}{\partial t}(\rho h) = \nabla \alpha_{eff} \nabla h, \tag{9}$$

where $\rho$, $h$ and $\alpha_{eff}$ are the density, enthalpy and effective thermal diffusivity of the solid, respectively.

## B. Implementation of multiRegionBYRFoam

The above governing equations are implemented with a new solver called multiRegionBYRFoam, which is an extended multi-region version of our in-house compressible flow solver BYRFoam [9], developed based on the framework of open-source software OpenFOAM. BYRFoam has been successfully used for modelling detonation combustion [10]. Multi-region solving capability is added to the original solver to evaluate the heat transfer between the flow field and RDC wall, with the aim of organizing proper thermal management for RDE. Developed at its early stage, this version of multiRegionBYRFoam can only solve single solid region and will be improved for multiple solid regions calculation in the future. The flowchart is illustrated on Figure 1. Note that the energy equations in fluid and solid regions are coupled at the interface in the following manner. The temperature and the heat flux on both sides of the interface should be equal, if a first order discretization of the temperature gradient is assumed, then the temperature on the patch for both sides can be calculated, and then they play the role as boundary conditions for fluid and solid regions respectively.

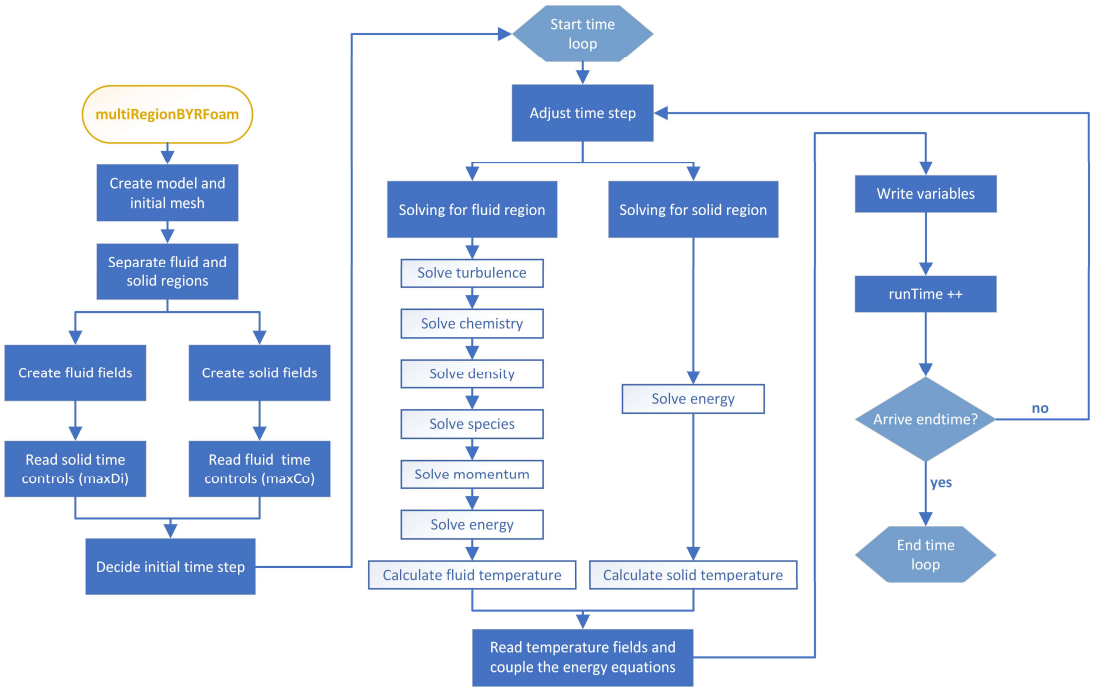


Figure 1: Solution procedure of multiRegionBYRFoam

## C. Computational model

Conjugate heat transfer simulations were performed for an annular combustion chamber with the outer chamber wall. The numerical domain contains 2.25 million structured cells in total, with cell size less than 0.2 mm. The number of solid cells is 0.63 million and fluid cells sum up to 1.62 million. The geometry and meshes for both fluid and solid regions are presented in Figure 2.

At the initial moment, the combustion chamber is filled with cold product (pressure 0.1 MPa and temperature 300 K). In this detonation-wall heat transfer problem, premixed $H_2$/air are asumed to inject into the chamber through converging micro-nozzles at each grid point on the inlet patch. A hot spot with pressure 2.5 MPa and temperature 2500 K, followed by a region of cold premixed $H_2$/air mixture at bottom of the chamber is set to initiate the detonation wave. The detailed $H_2$/air chemical reaction kinetic mechanism with 9 species and 19 elementary reactions proposed by Henry et al. [11] is used.

According to the previous study of Olcucuoglu et al. [8], the wall temperature is only slightly higher in the case with adiabatic outer wall boundary condition than in the case where constant heat flux is set to

approximate natural convection. In this study, the heat loss to the environment around the outer surface of the RDC is neglected and the adiabatic boundary condition is applied for the outer surface of the solid region. 304 stainless steel is selected as the outer chamber wall material. Its density, heat capacity $C_p$ and thermodynamic conductivity $k$ are 7900 kg/m$^3$, 477 J/(kg·K) and 14.9 W/(m·K), respectively.

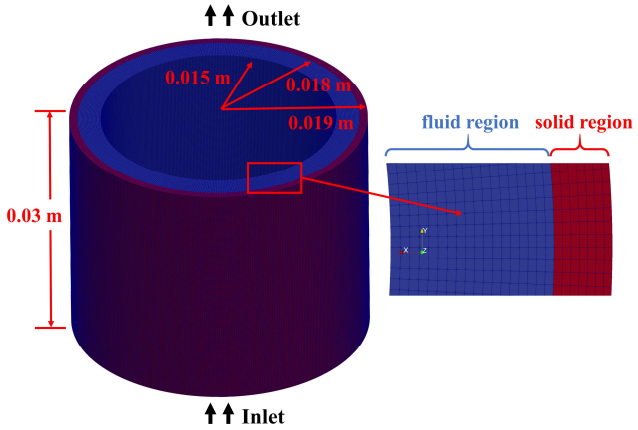


Figure 2: Computational domain and grids of RDC with solid wall

## 3 Results

The conputation time is restricted to 2 ms to save the calculation cost. Stable propagation of detonation waves has been achieved by this time. Although thermal equilibrium cannot be achieved after such short time, preliminary trends can be found on the thermal environment of RDC. In the case studied here, premixed hydrogen/air mixture with equivalence ratio of 1, total pressure 0.8 MPa and total temperature 360 K is injected into the combustor. The initial temperatures of fluid and solid regions are both 300K. Figure 3(a) shows the temperature contours of both gas and detonation chamber wall through the cross-section plot of the RDC. It can be seen that a single detonation is propagating circumferentially and the instantaneous gas temperature can be up to 3300 K.

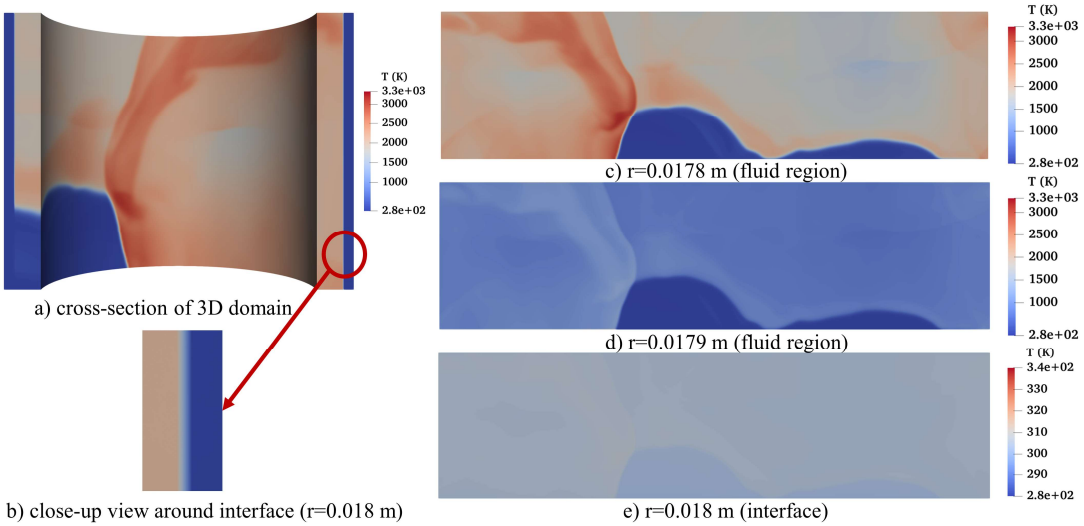


Figure 3: Spatial temperature distributions of the flow field and solid wall at $t$=2 ms. a) 3D view, b) close-up view of the interface, and c), d), e) 2D unwrapped view at different radical positions

Due to the relatively short run time, the temperature variations across the fluid-solid interface ($r$=0.018 m) is mild, and can be recognized by local enlarged Figure 3(b). Right at this interface, the temperature

slightly increased up to 307 K by the time of 2 ms, provided in the 2D unwrapped view in Figure 3(e). This temperature magnitude is consistent with the numerical results of Yelken et al. [12]. Besides, the clear effect of gas temperature on the instantaneous spatial distribution of wall temperature can also be seen. At $r$=0.0179 m section shown in Figure 3(d), which is contained inside the fluid region, the temperature ranges from 293 K to 2165 K. When it comes to the further section at $r$=0.0178 m demonstrated in Figure 3(c), the temperature almost fully recovers to the internal flow field condition, where the high temperature areas mainly distribute around rotating detonation wave and oblique shock wave, while the contact burning occurring at the interface of fresh reactant and detonation product also raises the local temperature.

To further investigate the temporal variation of wall temperature, four gauging points with the same azimuthal location and axial distance from the injection plate (z=0.01 m) but different radical positions $r$=0.0179 m, 0.018 m, 0.0181 m and 0.0182 m are set to monitor the time history of temperature between 1 ms~2 ms. As shown in Figure 4, the red curves represent the temperatures inside the solid wall, while the blue curves show the temperatures inside the fluid region. The initial sharp spikes are common shapes of detonation temperature waveform and indicate the passing single detonation wave. It should be noticed that the significant decrease of gas temperature starting from 1.35 ms is due to the injection of cold reactant, the height of which fluctuates with the pressure oscillations caused by the previous detonation wave as well as the collision between shock waves and injection wall [13], following the so-called self-adjusting mechanism [14]. Although the temperature rise of solid wall is mild, especially at $r$=0.0181 m, the rise and fall of temperature in fluid and solid regions are always synchronous, confirming the good coupling of the both sides.

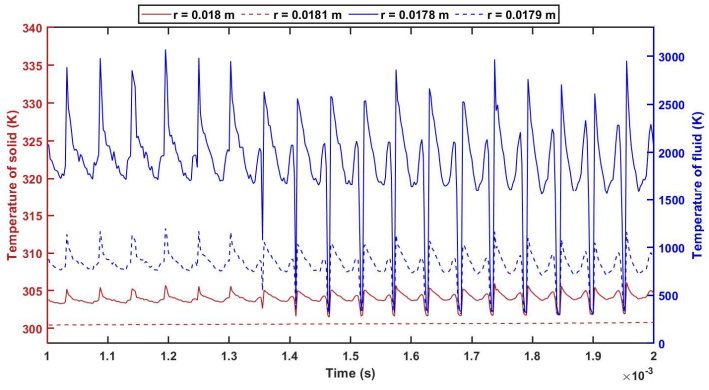


Figure 4: temporal variations of temperature at different radical positions

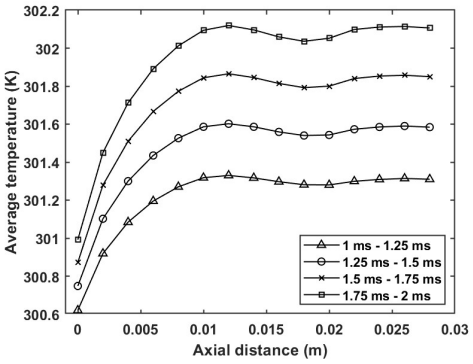


Figure 5: axial variations of circumferentially-averaged temperature within 4 time ranges

In consideration of the non-uniform distribution of instantaneous wall temperature shown in Figure 3(e), it is worthy to evaluate the variations of time-averaging temperature in order to organize proper cooling for engineering practice. Figure 5 provides the axial variations of the circumferentially-and-temporally-averaged temperature within four time ranges. The average temperature rises gradually as time goes by, and all follow the same axial variation trend, i.e., the fill zone adjacent to the head wall is cooled by the injected reactant, then the temperature rises to the maximum near the triple point of rotating detonation (around 0.01 m in this case). After a period of reduction, the temperature achieves another peak value owing to the oblique shock wave. The above trend is consistent with the experimental results of Bykovskii et al. [1], as well as the numerical results of Roy et al. [4]. This indicates that both areas near triple points and oblique shocks should receive enhanced cooling, while the certain distance above the head wall may be effectively cooled through adjusting the non-premixed injection manners.

## 4 Conclusions

The conjugate heat transfer problem between the RDC flow field and chamber wall was calculated utilizing the newly developed multi-region solver multiRegionBYRFoam, to fill the gap of fully coupled fluid-to-solid heat transfer simulation for rotating detonation chamber. The solution procedure and coupling method of the new solver were clarified. Then the radical, axial and temporal variations of RDC wall temperature in a single-wave case solved by multiRegionBYRFoam were analyzed. The fluid and solid regions are well coupled, and the maximal axial wall temperature was found to occur near the triple points and oblique shocks. This investigation provides insight into the transient heat load of rotating detonation chamber wall, and offers reference for thermal management of RDE and the efficient cooling considerations in the near future. Future work includes long duration simulation that equilibrium wall temperature can be achieved, and the study of effects of mass flow rate, equivalence ratio and chamber geometry on the thermal environment of RDE.

## References

[1] Bykovskii FA. Thermal fluxes in combustion chamber walls in the detonation and turbulent combustion modes. Combustion, Explosion and Shock Waves. 1991; 27:66-71.

[2] Theuerkauf SW, Schauer FR, Anthony R, Hoke JL, 2015. Experimental Characterization of High-Frequency Heat Flux in a Rotating Detonation Engine.

[3] Theuerkauf SW, Schauer FR, Anthony R, Paxson DE, Stevens CA, Hoke JL, 2016. Comparison of Simulated and Measured Instantaneous Heat Flux in a Rotating Detonation Engine.

[4] Roy A, Bedick C, Strakey P, Sidwell T, Ferguson D, Sisler A, et al., 2016. Development of a Three-dimensional Transient Wall Heat Transfer Model of a Rotating Detonation Combustor.

[5] Cocks PAT, Holley AT, Greene CB, Haas M. Development of a high fidelity RDE simulation capability., 53rd AIAA Aerospace Sciences Meeting2015.

[6] Wang Y, Wang J, Qiao W. Effects of thermal wall conditions on rotating detonation. COMPUT FLUIDS. 2016; 140:59-71.

[7] Wu K, Zhang L, Luan M, Wang J. Effects of Isothermal Wall Boundary Conditions on Rotating Detonation Engine. COMBUST SCI TECHNOL. 2021; 193:211-24.

[8] Olcucuoglu B, Temel O, Tuncer O, Saracoglu BH, 2018. A Novel Open Source Conjugate Heat Transfer Solver for Detonation Engine Simulations.

[9] Xia Z, Sheng Z, Shen D, Wang J. Numerical investigation of pre-detonator in rotating detonation engine. INT J HYDROGEN ENERG. 2021; 46:31428-38.

[10] Sheng Z, Cheng M, Shen D, Wang JP. An active direction control method in rotating detonation combustor. INT J HYDROGEN ENERG. 2022; 47:23427-43.

[11] Ó Conaire M, Curran HJ, Simmie JM, Pitz WJ, Westbrook CK. A comprehensive modeling study of hydrogen oxidation. INT J CHEM KINET. 2004; 36:603-22.

[12] Yelken U, Tuncer O, Saracoglu BH, 2019. Conjugate heat transfer analysis of rotating detonation engines.

[13] Zhang S, Yao S, Luan M, Zhang L, Wang J. Effects of injection conditions on the stability of rotating detonation waves. SHOCK WAVES. 2018; 28:1079-87.

[14] Liu Y, Wang Y, Li Y, Li Y, Wang J. Spectral analysis and self-adjusting mechanism for oscillation phenomenon in hydrogen-oxygen continuously rotating detonation engine. CHINESE J AERONAUT. 2015; 28:669-75.